

Electronic supplementary materials *Mendeleev Commun.*, 2019, **29**, 150–152

## Synthesis and structure of stereoisomers of 3,4-benzo-5,10-diphenyl-1,3-diaza-7-oxa-6-phosphabicyclo[4.3.1]decane-2,6-dione

Mudaris N. Dimukhametov, Gulnara A. Ivkova, Igor A. Litvinov, Robert R. Fayzullin, Khasan R. Khayarov and Vladimir F. Mironov

### Table of contents

Electronic supplementary information	
General remarks	S2
Figure S1. Geometry of diastereoisomer <b>4</b> ( <i>d</i> <sub>1</sub> , P <sub>R</sub> C <sub>R</sub> /P <sub>S</sub> C <sub>S</sub> ) in the crystal, P <sub>R</sub> C <sub>R</sub> -enantiomer is shown.	S2
Figure S2. Geometry of diastereoisomer <b>4</b> ( <i>d</i> <sub>2</sub> , P <sub>S</sub> C <sub>R</sub> /P <sub>R</sub> C <sub>S</sub> ) in the crystal, P <sub>S</sub> C <sub>R</sub> -enantiomer is shown.	S2
Figure S3. <sup>31</sup> P- <sup>1</sup> H and <sup>31</sup> P NMR spectra (162.0 MHz, CDCl <sub>3</sub> ) of compound <b>4</b> ( <i>d</i> <sub>1</sub> ).	S3
Figure S4. <sup>1</sup> H NMR spectrum (400 MHz, CDCl <sub>3</sub> ) of compound <b>4</b> ( <i>d</i> <sub>1</sub> ).	S4
Figure S5. <sup>1</sup> H NMR (red) and <sup>1</sup> H- <sup>31</sup> P spectra (400 MHz, CDCl <sub>3</sub> ) of compound <b>4</b> ( <i>d</i> <sub>1</sub> ).	S5
Figure S6. <sup>13</sup> C- <sup>1</sup> H NMR spectrum (100.6 MHz, CDCl <sub>3</sub> ) of compound <b>4</b> ( <i>d</i> <sub>1</sub> ).	S6
Figure S7. <sup>13</sup> C NMR spectrum (100.6 MHz, CDCl <sub>3</sub> ) of compound <b>4</b> ( <i>d</i> <sub>1</sub> ).	S7
Figure S8. 123-134 ppm region of <sup>13</sup> C NMR spectrum (100.6 MHz, CDCl <sub>3</sub> ) of compound <b>4</b> ( <i>d</i> <sub>1</sub> ).	S8
Figure S9. <sup>13</sup> C and <sup>13</sup> C- <sup>1</sup> H NMR spectra (100.6 MHz, CDCl <sub>3</sub> ) of compound <b>4</b> ( <i>d</i> <sub>1</sub> ).	S9
Figure S10. Fragments of <sup>13</sup> C and <sup>13</sup> C- <sup>1</sup> H NMR spectra (100.6 MHz, CDCl <sub>3</sub> ) of compound <b>4</b> ( <i>d</i> <sub>1</sub> ).	S10
Figure S11. 123-134 ppm region of <sup>13</sup> C and <sup>13</sup> C- <sup>1</sup> H NMR spectra (100.6 MHz, CDCl <sub>3</sub> ) of compound <b>4</b> ( <i>d</i> <sub>1</sub> ).	S11
Figure S12. High-field regions of <sup>13</sup> C and <sup>13</sup> C- <sup>1</sup> H NMR spectra (100.6 MHz, CDCl <sub>3</sub> ) of compound <b>4</b> ( <i>d</i> <sub>1</sub> ).	S12
Figure S13. <sup>31</sup> P NMR spectrum (162.0 MHz, CDCl <sub>3</sub> ) of compound <b>4</b> ( <i>d</i> <sub>2</sub> ).	S13
Figure S14. <sup>1</sup> H NMR spectrum (400 MHz, CDCl <sub>3</sub> ) of compound <b>4</b> ( <i>d</i> <sub>2</sub> ).	S14
Figure S15. <sup>13</sup> C- <sup>1</sup> H NMR spectrum (100.6 MHz, CDCl <sub>3</sub> ) of compound <b>4</b> ( <i>d</i> <sub>2</sub> ).	S15
Figure S16. <sup>13</sup> C NMR spectrum (100.6 MHz, CDCl <sub>3</sub> ) of compound <b>4</b> ( <i>d</i> <sub>2</sub> ).	S16
Figure S17. 123-134 ppm region of <sup>13</sup> C NMR spectrum (100.6 MHz, CDCl <sub>3</sub> ) of compound <b>4</b> ( <i>d</i> <sub>2</sub> ).	S17
Figure S18. <sup>13</sup> C and <sup>13</sup> C- <sup>1</sup> H NMR spectra (100.6 MHz, CDCl <sub>3</sub> ) of compound <b>4</b> ( <i>d</i> <sub>2</sub> ).	S18
Figure S19. 123-143 ppm region of <sup>13</sup> C and <sup>13</sup> C- <sup>1</sup> H NMR spectra (100.6 MHz, CDCl <sub>3</sub> ) of compound <b>4</b> ( <i>d</i> <sub>2</sub> ).	S19
Figure S20. High-field regions of <sup>13</sup> C and <sup>13</sup> C- <sup>1</sup> H NMR spectra (100.6 MHz, CDCl <sub>3</sub> ) of compound <b>4</b> ( <i>d</i> <sub>2</sub> ).	S20

**General remarks.** NMR spectra were recorded on a Bruker Avance-400 instrument (400 MHz,  $^1\text{H}$ ; 161.0 MHz,  $^{31}\text{P}$ ; and 100.6 MHz,  $^{13}\text{C}$ ) in  $\text{CDCl}_3$  relative to the residual signals of the solvent. Mass spectra (EI) were taken on a DFS Thermo Electron Corporation instrument (Germany). The energy of ionizing electrons was 70 eV, the temperature of the ion source was  $290^\circ\text{C}$ , a system of direct input of the sample into the ion source was used, temperature of the evaporator was  $250^\circ\text{C}$ . Elemental analysis was performed on a EuroVector-3000 instrument (C, H, N) or manually by pyrolysis in an oxygen stream (P).

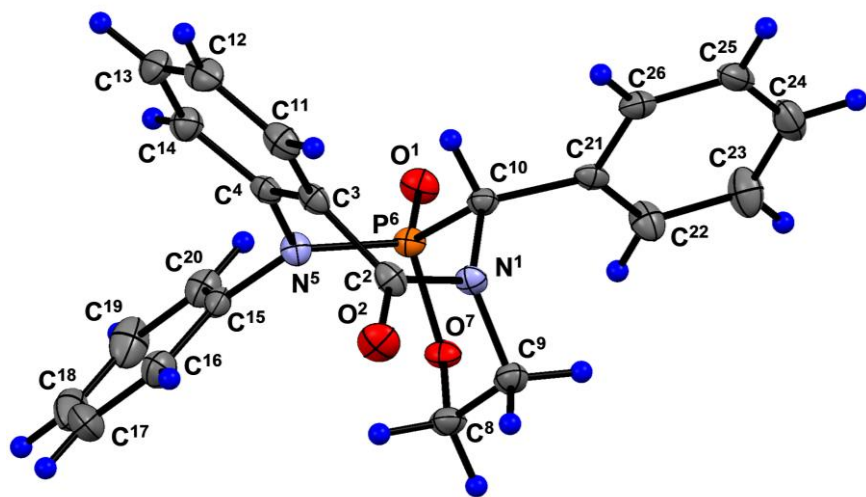


**Figure S1.** Geometry of diastereoisomer **4** ( $d_1$ ,  $P_R C_R/P_S C_S$ ) in the crystal,  $P_R C_R$ -enantiomer is shown (hereafter non-hydrogen atoms are presented as thermal ellipsoids with 50% probability). Selected bond lengths ( $\text{\AA}$ ), bond and torsion angles (deg):  $\text{P}^6\text{-O}^1$  1.461(2),  $\text{P}^6\text{-O}^7$  1.586(2),  $\text{P}^6\text{-N}^5$  1.674(2),  $\text{P}^6\text{-C}^{10}$  1.805(3),  $\text{O}^2\text{-C}^2$  1.225(3),  $\text{N}^1\text{-C}^2$  1.372(3),  $\text{N}^1\text{-C}^{10}$  1.477(3),  $\text{N}^5\text{-C}^4$  1.441(3),  $\text{O}^1\text{-P}^6\text{-O}^7$  110.5(1),  $\text{O}^1\text{-P}^6\text{-N}^5$  117.9(1),  $\text{O}^1\text{-P}^6\text{-C}^{10}$  117.5(1),  $\text{O}^7\text{-P}^6\text{-N}^5$  105.01(9),  $\text{O}^7\text{-P}^6\text{-C}^{10}$  103.8(1),  $\text{N}^5\text{-P}^6\text{-C}^{10}$  100.5(1),  $\text{P}^6\text{-O}^7\text{-C}^8$  119.7(1),  $\text{P}^6\text{-C}^{10}\text{-N}^1$  105.5(2),  $\text{O}^1\text{-P}^6\text{-O}^7\text{-C}^8$  174.4(2),  $\text{O}^1\text{-P}^6\text{-N}^5\text{-C}^4$  -102.0(2),  $\text{O}^2\text{-C}^2\text{-C}^3\text{-C}^{11}$  52.2(4),  $\text{C}^{10}\text{-P}^6\text{-N}^5\text{-C}^4$  27.0(2),  $\text{C}^9\text{-N}^1\text{-C}^2\text{-O}^2$  32.9(3),  $\text{C}^2\text{-N}^1\text{-C}^{10}\text{-P}^6$  -85.3(2).

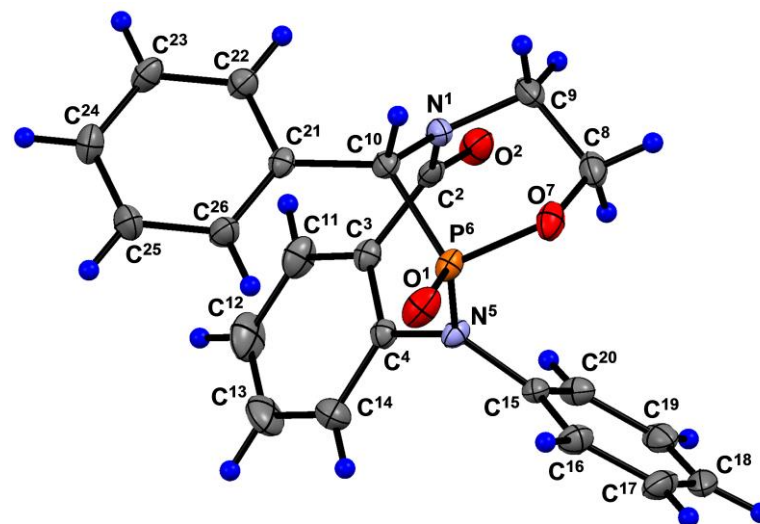


**Figure S2.** Geometry of diastereoisomer **4** ( $d_2$ ,  $P_S C_R/P_R C_S$ ) in the crystal,  $P_S C_R$ -enantiomer is shown. Selected bond lengths ( $\text{\AA}$ ) and bond and torsion angles (deg):  $\text{P}^6\text{-O}^1$  1.462(1),  $\text{P}^6\text{-O}^7$  1.596(1),  $\text{P}^6\text{-N}^5$  1.667(1),  $\text{P}^6\text{-C}^{10}$  1.814(2),  $\text{O}^2\text{-C}^2$  1.226(2),  $\text{N}^1\text{-C}^2$  1.365(2),  $\text{N}^1\text{-C}^{10}$  1.474(2),  $\text{N}^5\text{-C}^4$  1.439(2),  $\text{O}^1\text{-P}^6\text{-O}^7$  109.66(7),  $\text{O}^1\text{-P}^6\text{-N}^5$  117.86(7),  $\text{O}^1\text{-P}^6\text{-C}^{10}$  118.49(7),  $\text{O}^7\text{-P}^6\text{-N}^5$  105.20(6),  $\text{O}^7\text{-P}^6\text{-C}^{10}$  99.95(7),  $\text{N}^5\text{-P}^6\text{-C}^{10}$  103.53(6),  $\text{P}^6\text{-O}^7\text{-C}^8$  121.3(1),  $\text{P}^6\text{-C}^{10}\text{-N}^1$  104.52(9),  $\text{O}^1\text{-P}^6\text{-O}^7\text{-C}^8$  -176.2(1),  $\text{O}^1\text{-P}^6\text{-N}^5\text{-C}^4$  102.3(1),  $\text{O}^2\text{-C}^2\text{-C}^3\text{-C}^{11}$  -54.7(2),  $\text{C}^{10}\text{-P}^6\text{-N}^5\text{-C}^4$  -30.8(1),  $\text{C}^9\text{-N}^1\text{-C}^2\text{-O}^2$  -30.6(2),  $\text{C}^2\text{-N}^1\text{-C}^{10}\text{-P}^6$  80.2(1).

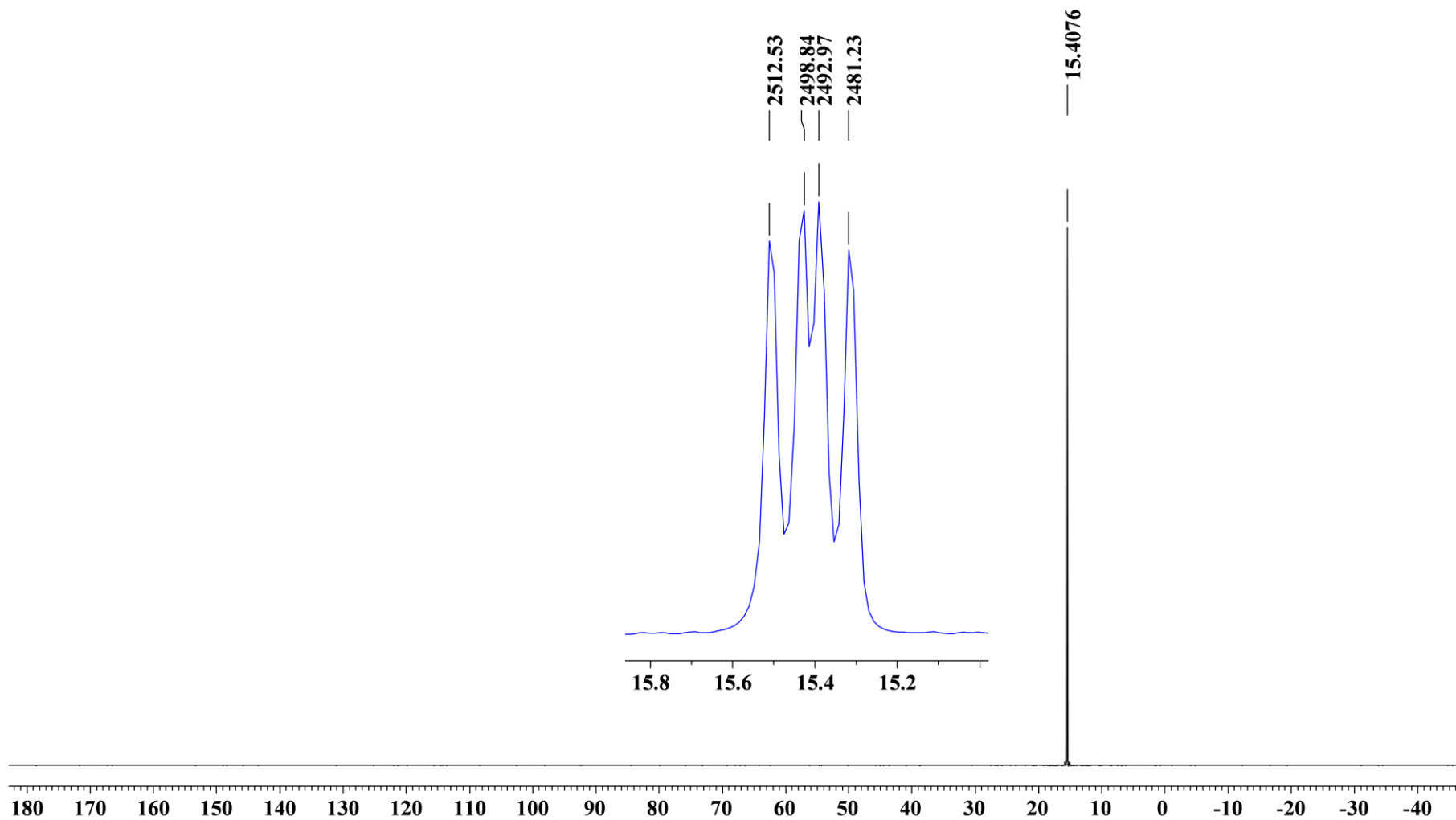


Figure S3.  $^{31}\text{P}$ - $\{^1\text{H}\}$  and  $^{31}\text{P}$  NMR spectra (162.0 MHz,  $\text{CDCl}_3$ ) of compound **4**( $d_1$ ).

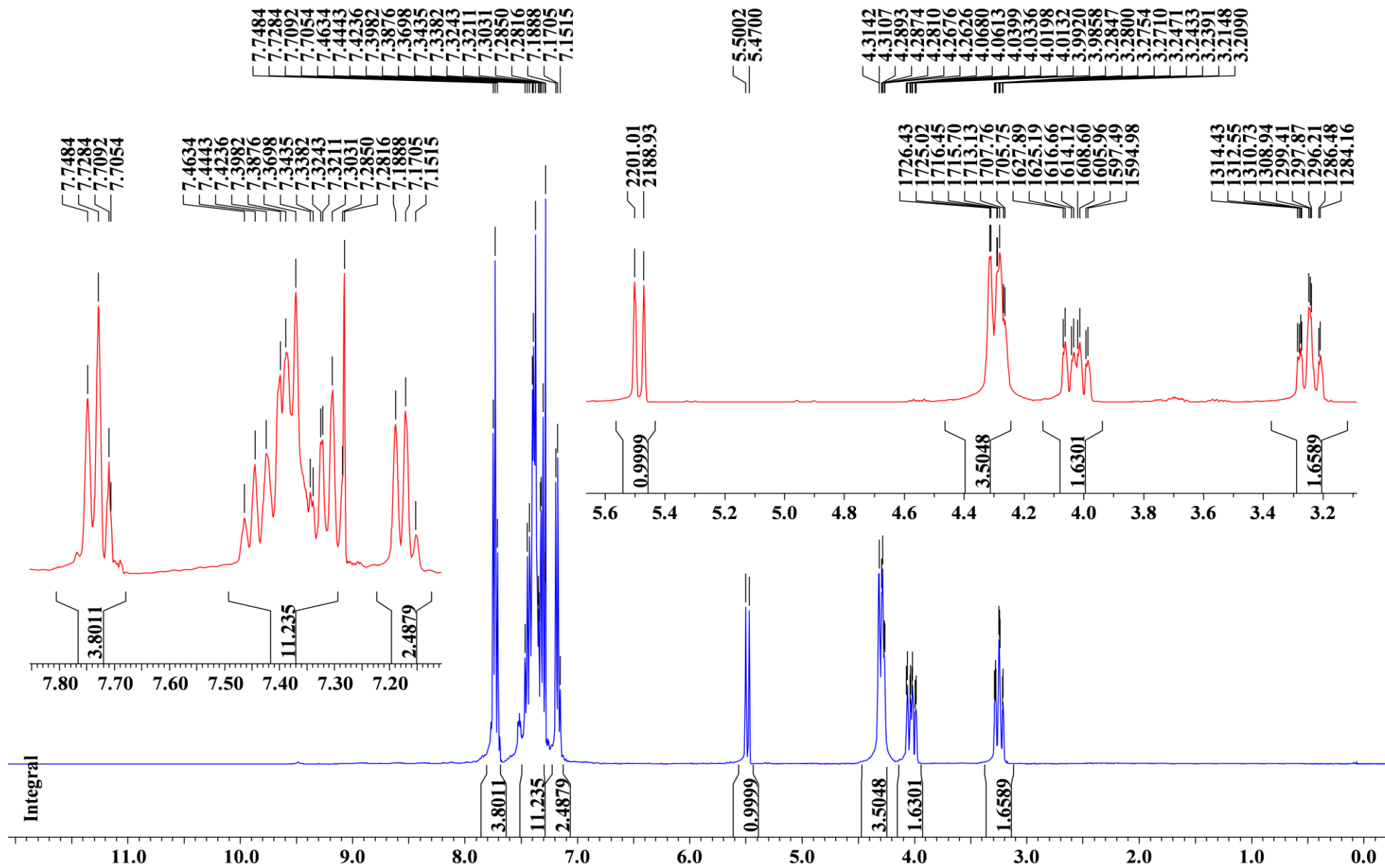


Figure S4.  $^1\text{H}$  NMR spectrum (400 MHz,  $\text{CDCl}_3$ ) of compound  $4(d_1)$ .

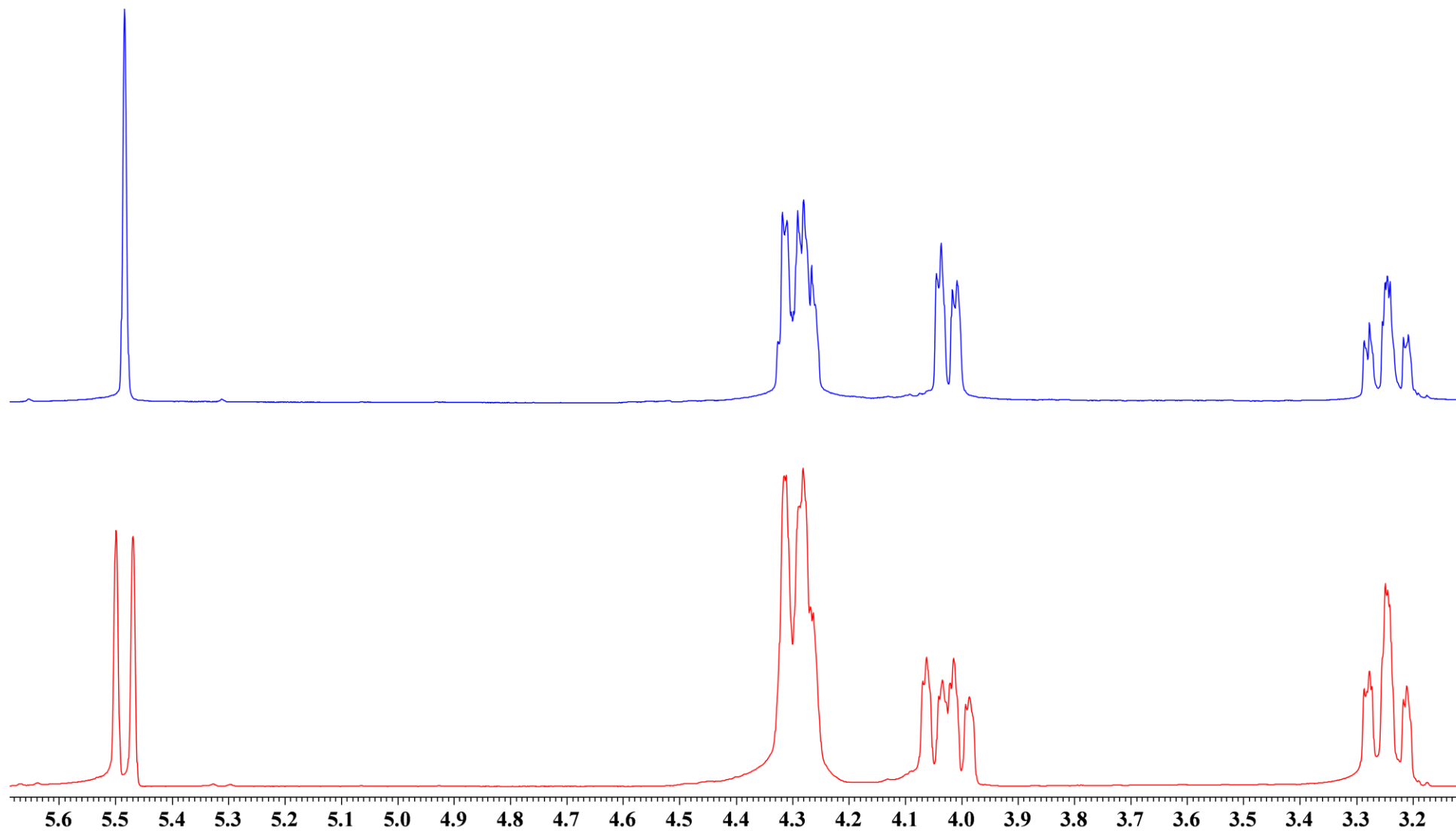


Figure S5.  $^1\text{H}$  NMR (red) and  $^1\text{H}$ - $\{^{31}\text{P}\}$  spectra (400 MHz,  $\text{CDCl}_3$ ) of compound **4**(*d*<sub>1</sub>).

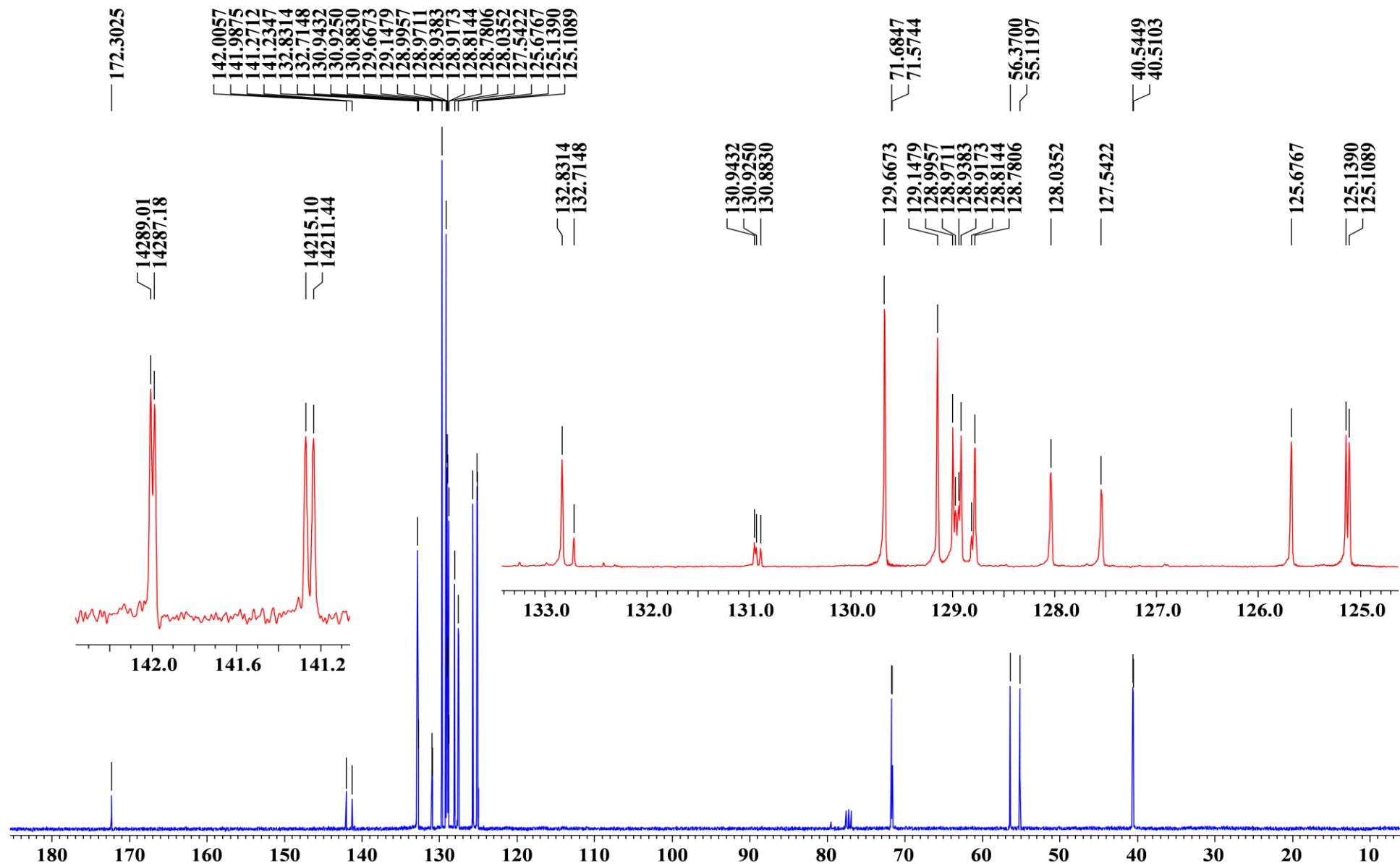
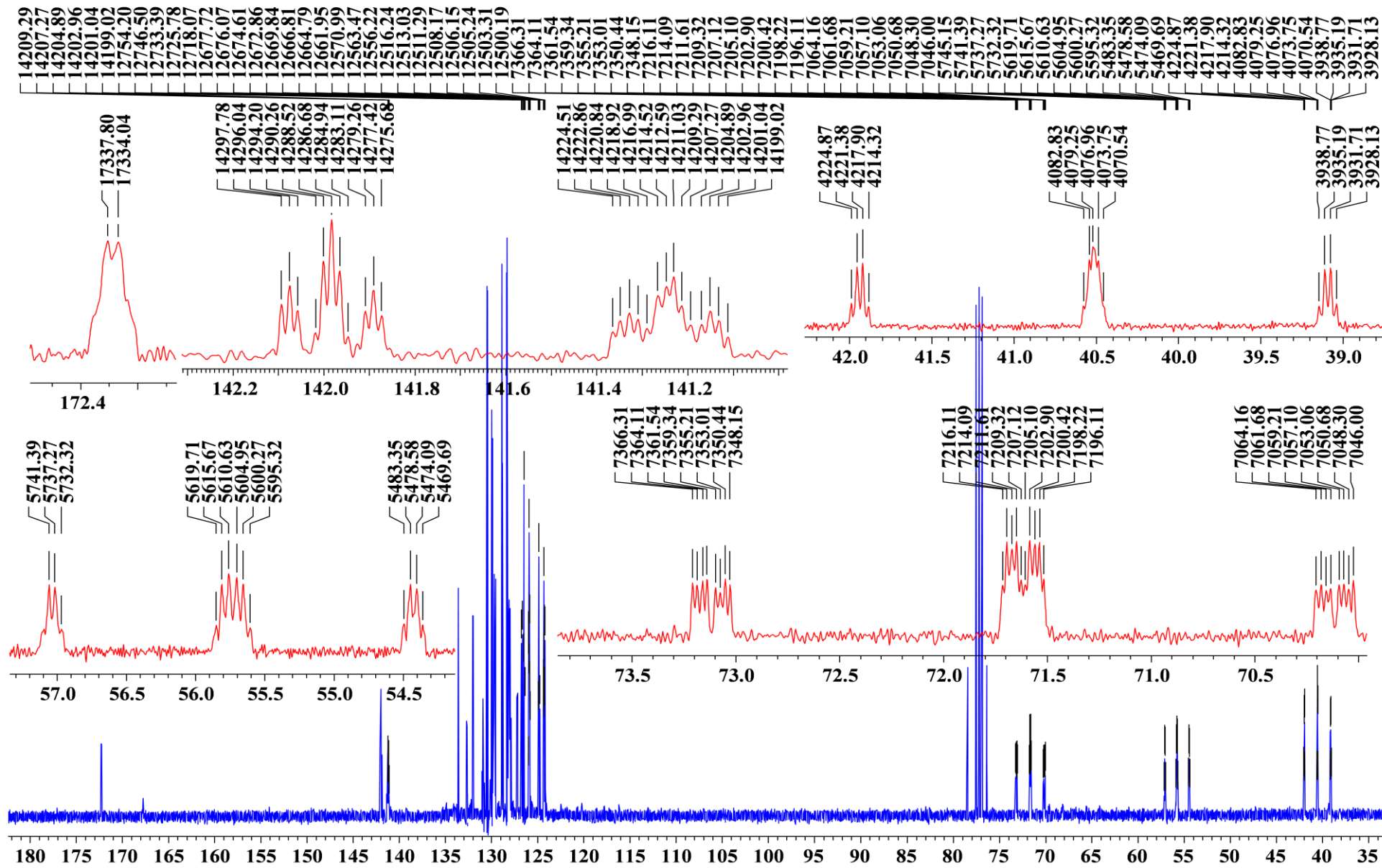


Figure S6.  $^{13}\text{C}$ - $\{^1\text{H}\}$  NMR spectrum (100.6 MHz,  $\text{CDCl}_3$ ) of compound  $4(d_1)$ .



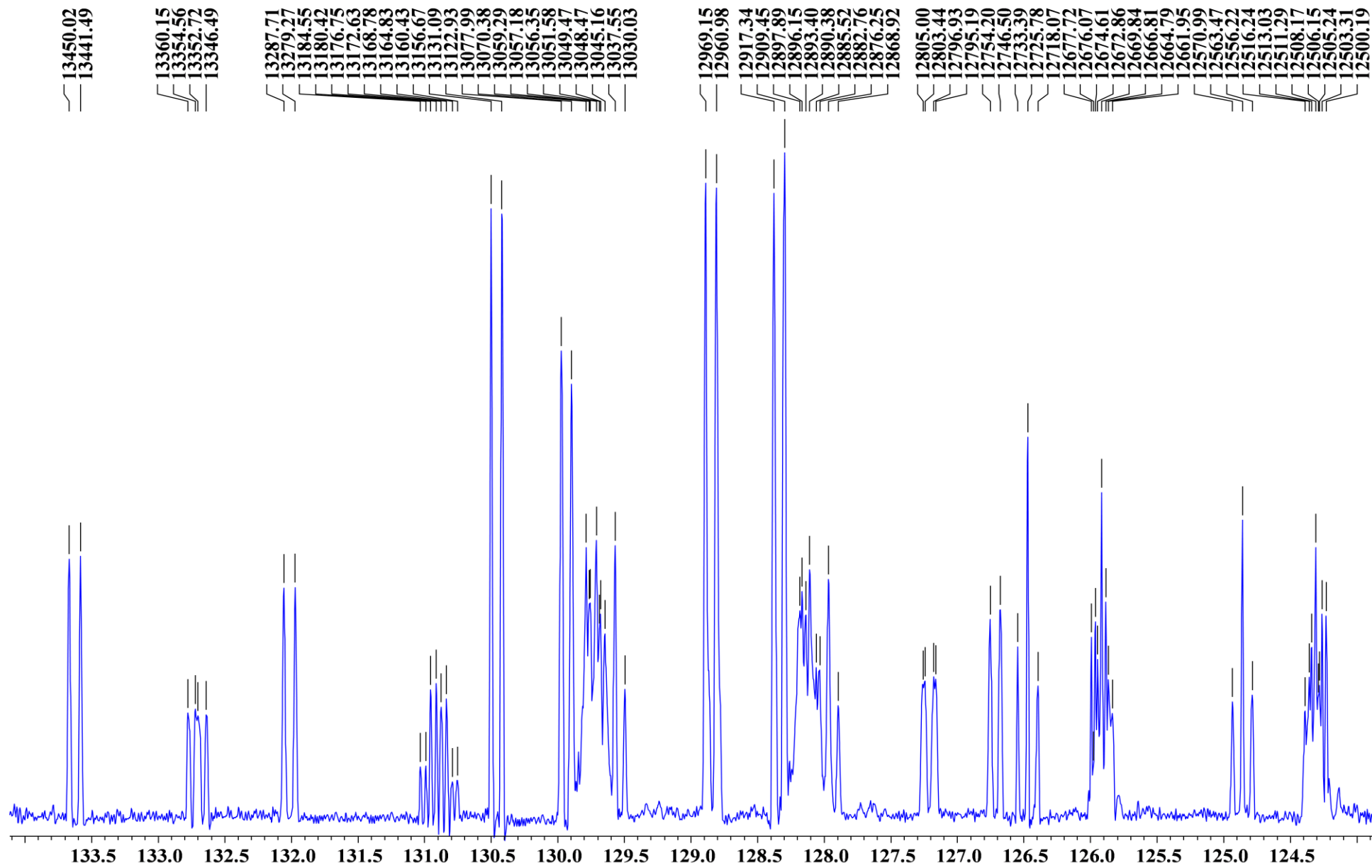


Figure S8. 123-134 ppm region of  $^{13}\text{C}$  NMR spectrum (100.6 MHz,  $\text{CDCl}_3$ ) of compound  $4(d_1)$ .

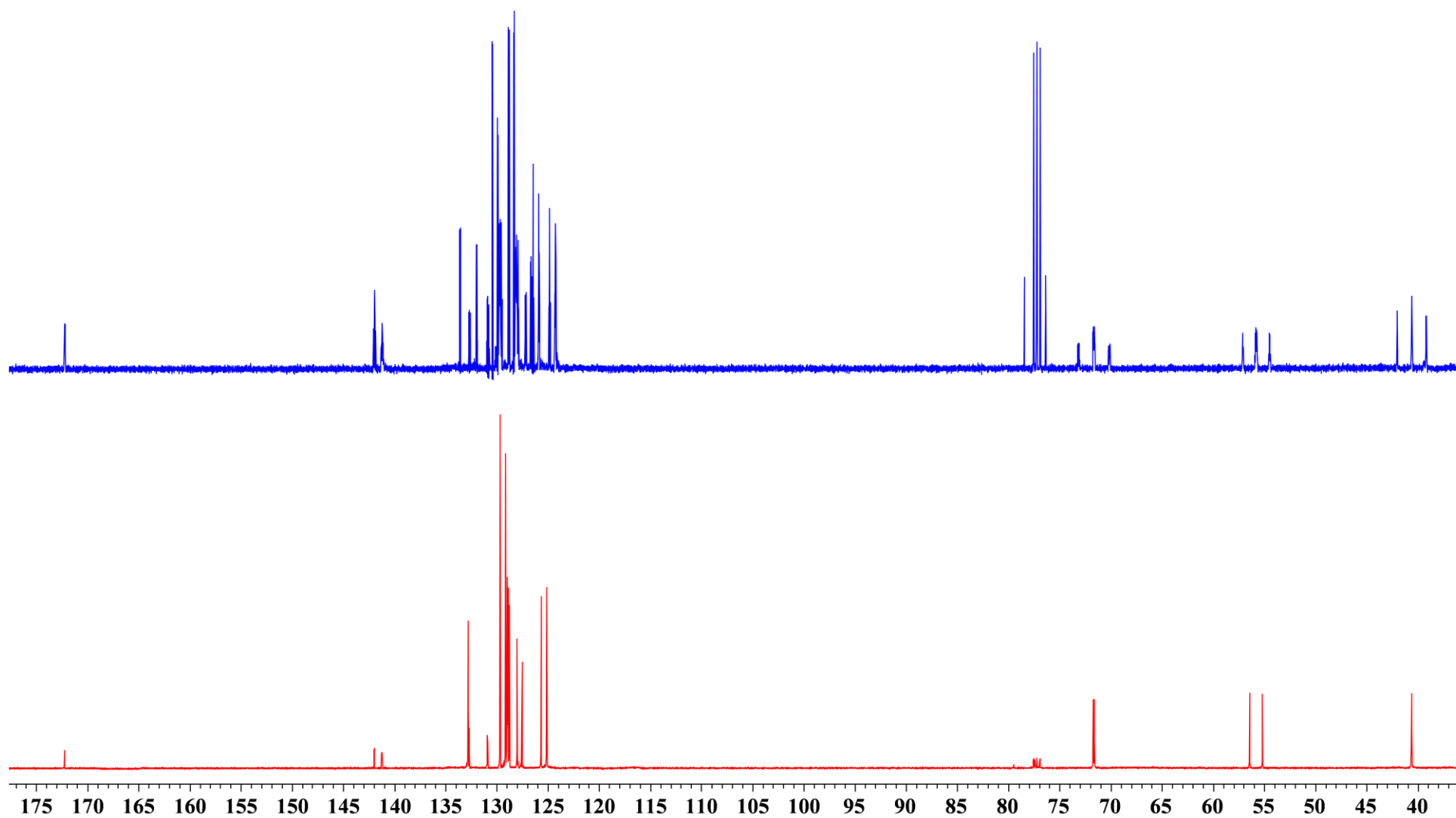


Figure S9. <sup>13</sup>C and <sup>13</sup>C-{<sup>1</sup>H} NMR spectra (100.6 MHz, CDCl<sub>3</sub>) of compound 4(d<sub>1</sub>).

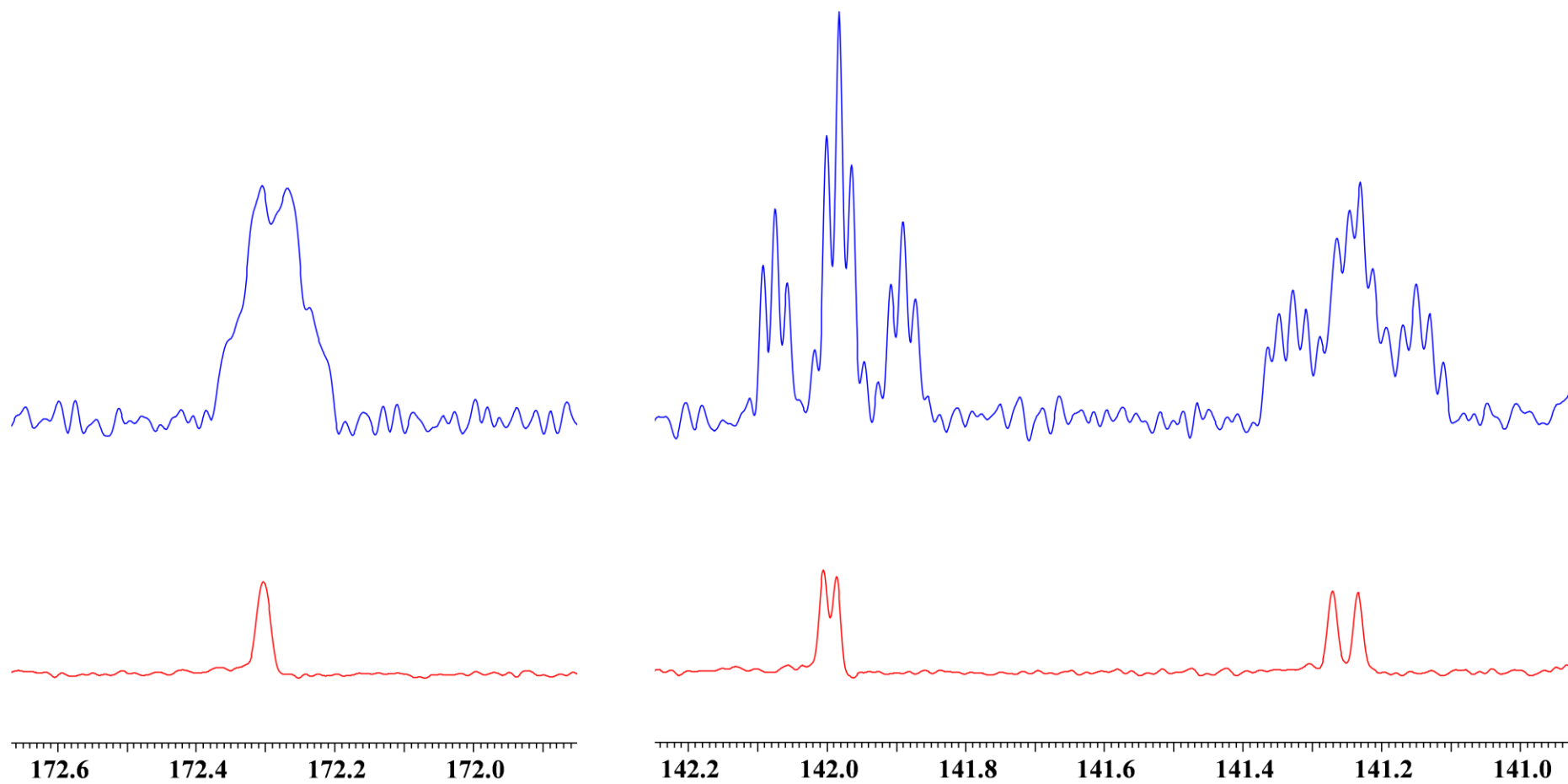


Figure S10. Fragments of <sup>13</sup>C and <sup>13</sup>C-{<sup>1</sup>H} NMR spectra (100.6 MHz, CDCl<sub>3</sub>) of compound 4(*d*<sub>1</sub>).

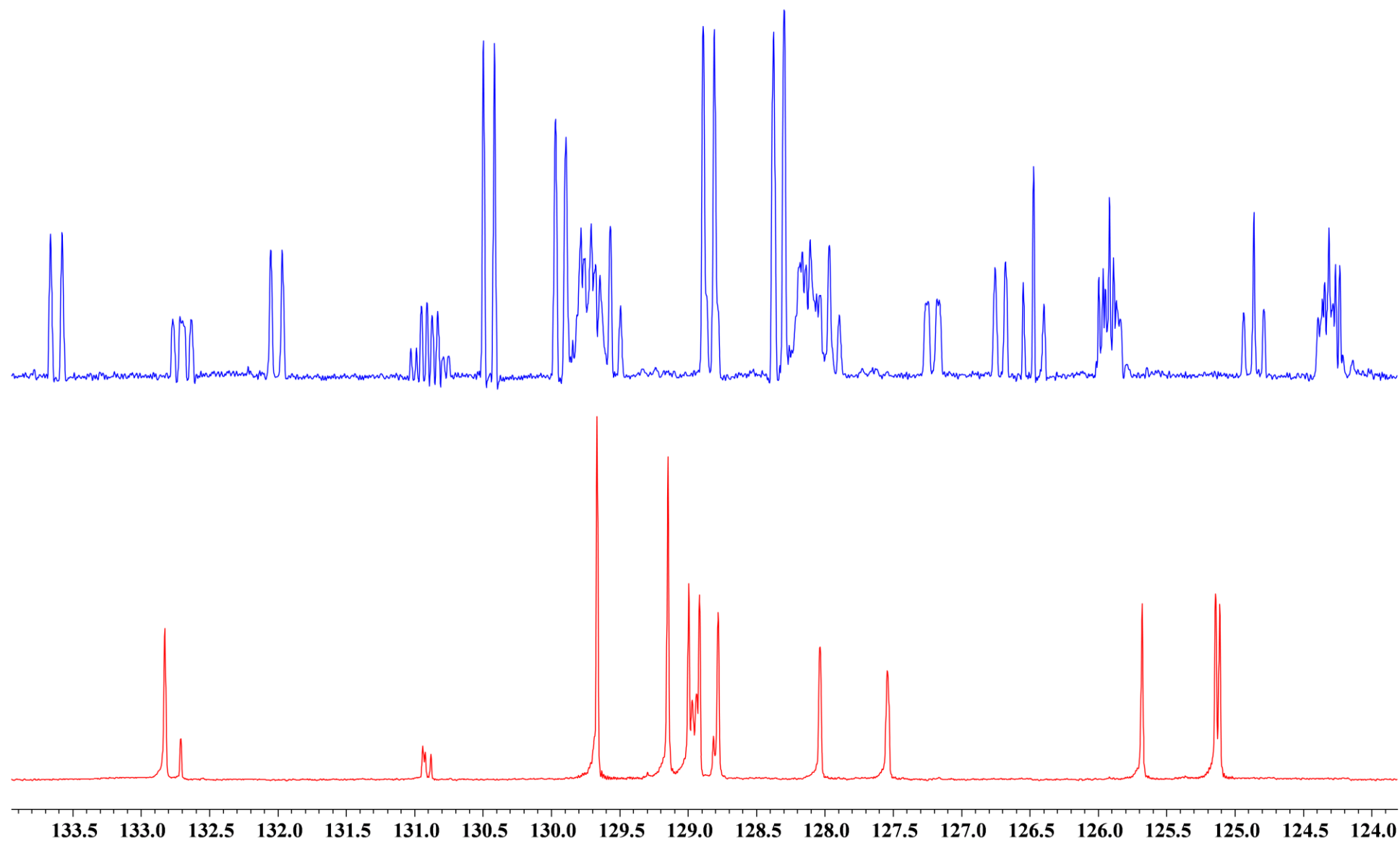


Figure S11. 123-134 ppm region of <sup>13</sup>C and <sup>13</sup>C-{<sup>1</sup>H} NMR spectra (100.6 MHz, CDCl<sub>3</sub>) of compound 4(*d*<sub>1</sub>).

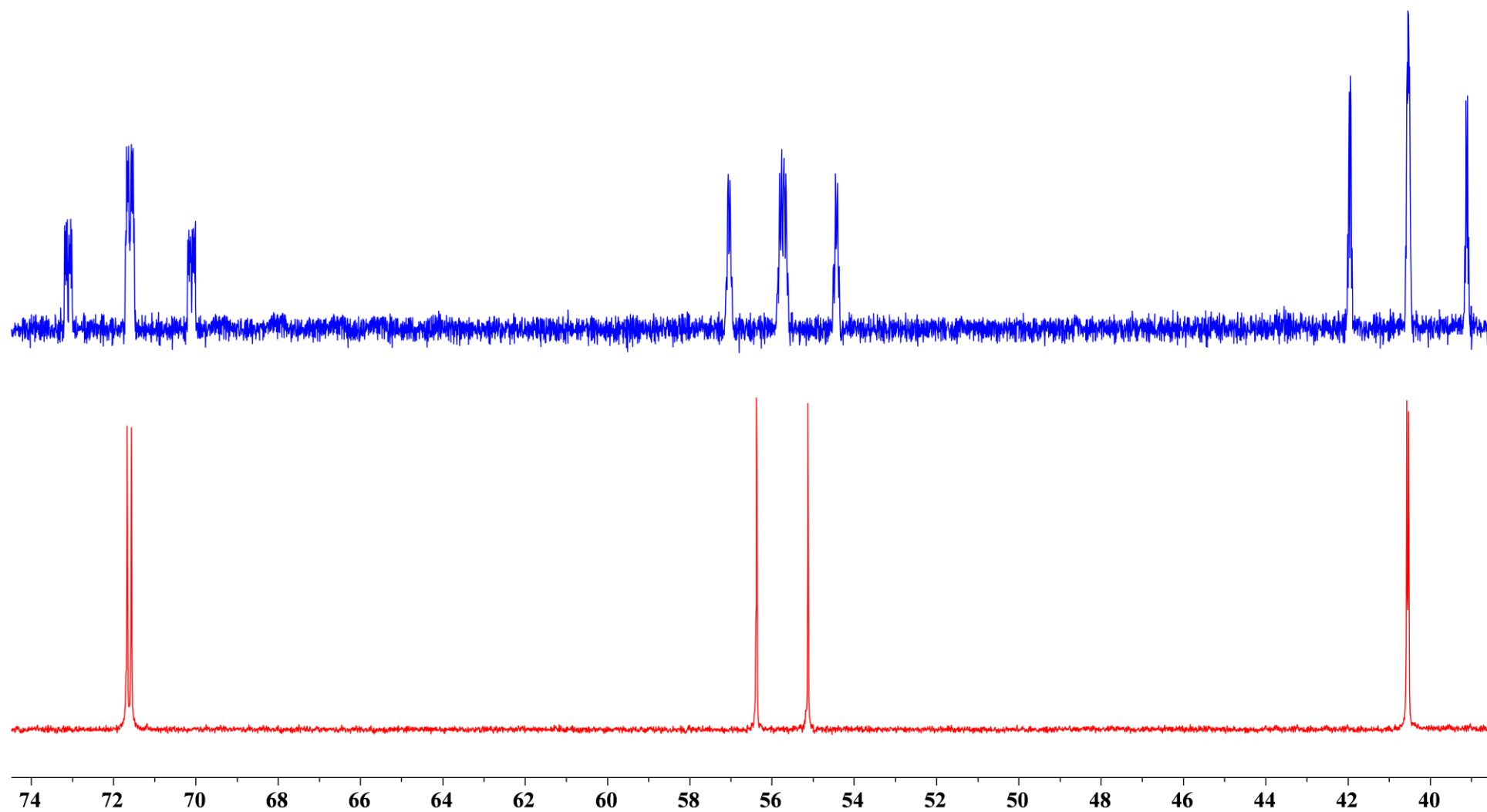


Figure S12. High-field regions of <sup>13</sup>C and <sup>13</sup>C-{<sup>1</sup>H} NMR spectra (100.6 MHz, CDCl<sub>3</sub>) of compound 4(*d*<sub>1</sub>).

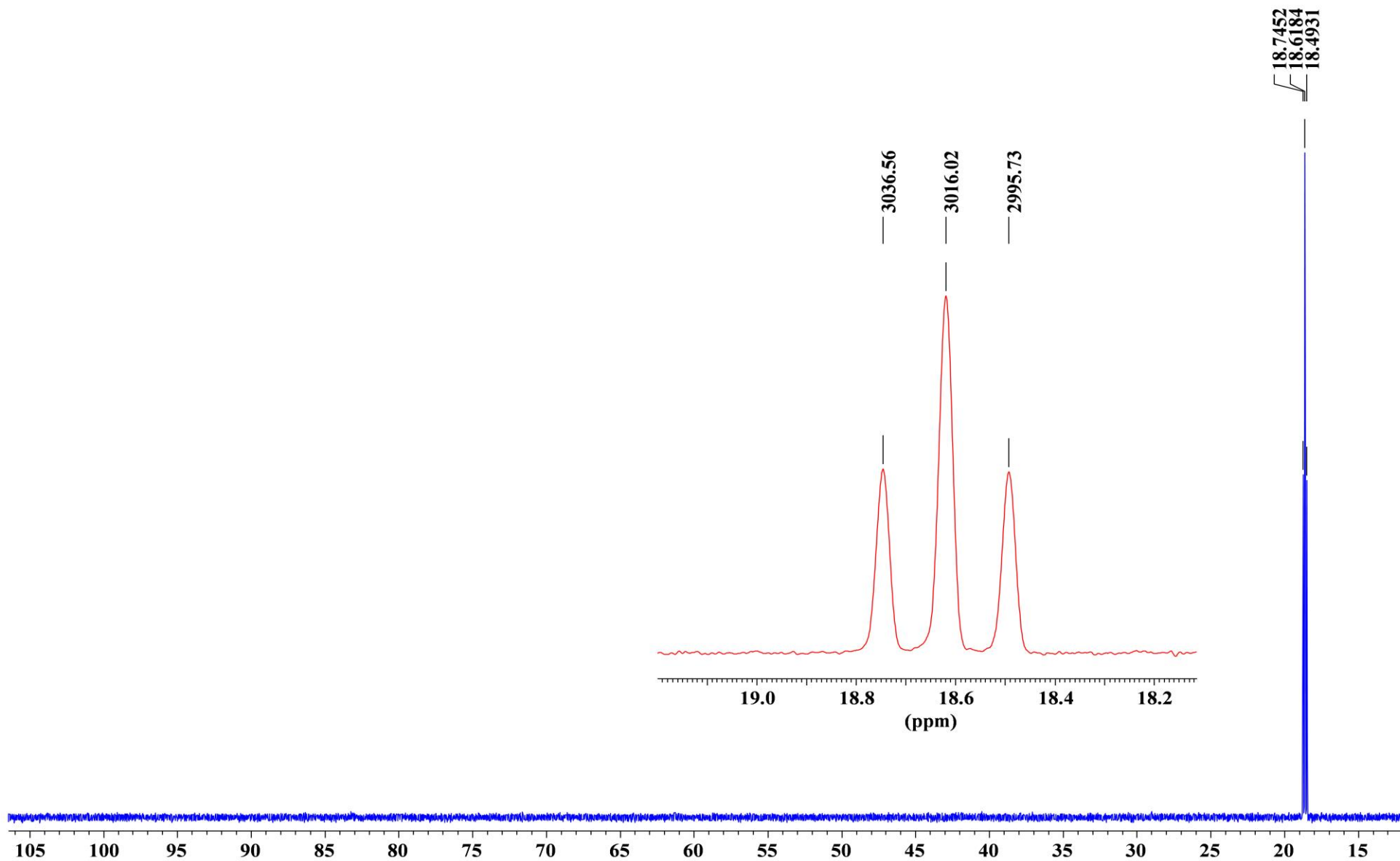


Figure S13.  $^{31}\text{P}$  NMR spectrum (162.0 MHz,  $\text{CDCl}_3$ ) of compound  $4(d_2)$ .

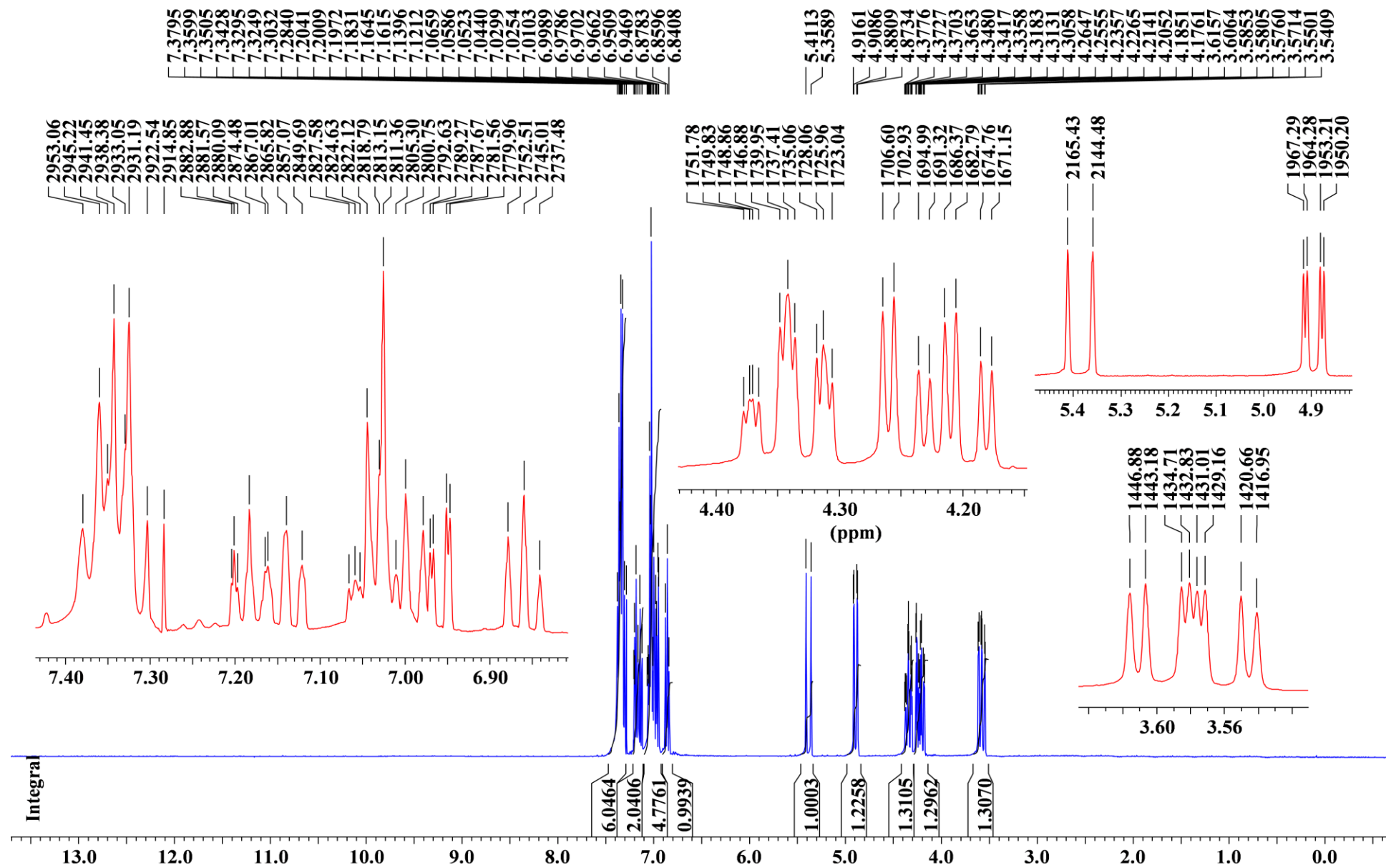
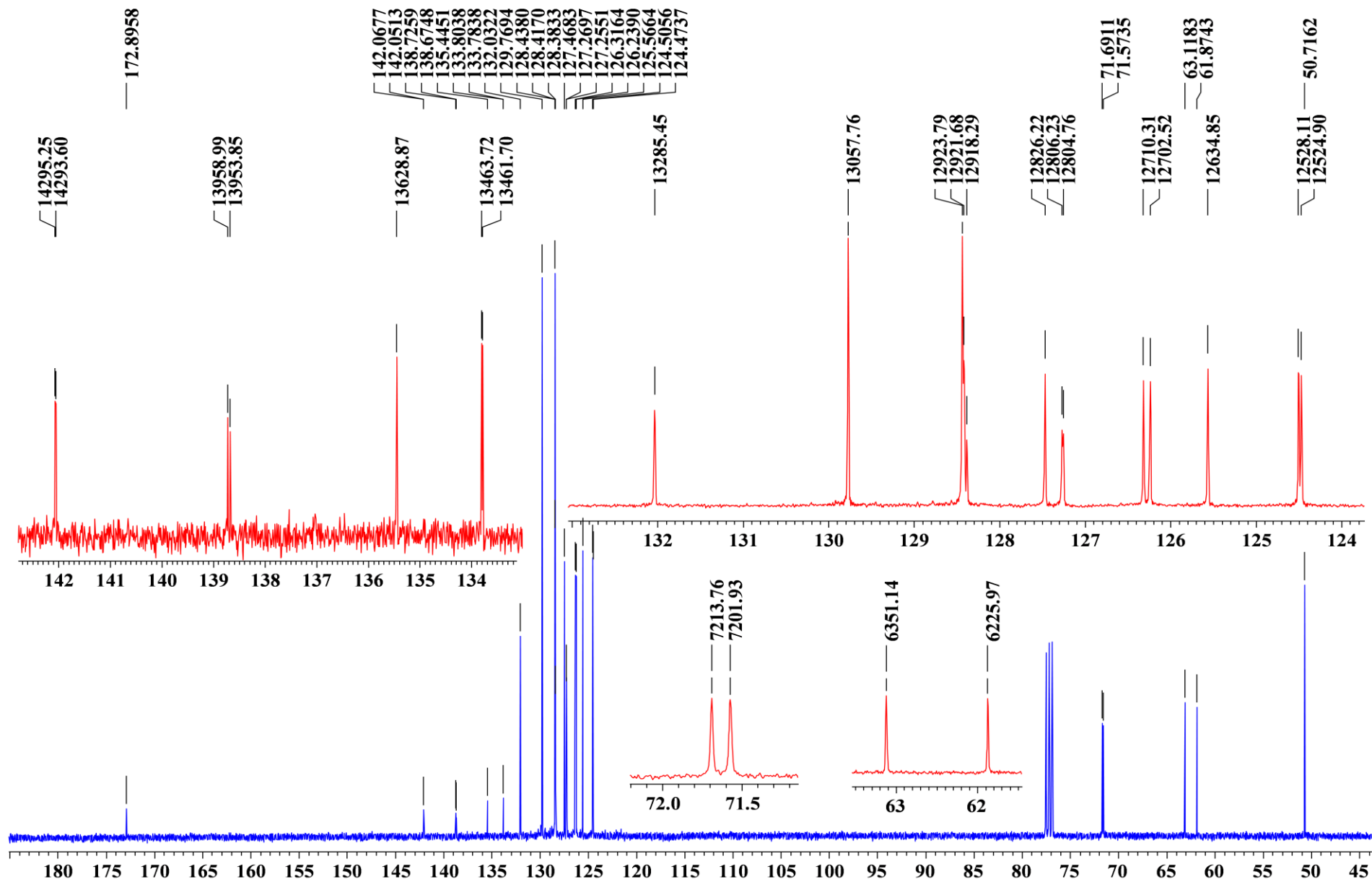


Figure S14.  $^1\text{H}$  NMR spectrum (400 MHz,  $\text{CDCl}_3$ ) of compound  $4(d_2)$ .

Figure S15.  $^{13}\text{C}$ - $\{^1\text{H}\}$  NMR spectrum (100.6 MHz,  $\text{CDCl}_3$ ) of compound  $4(d_2)$ .

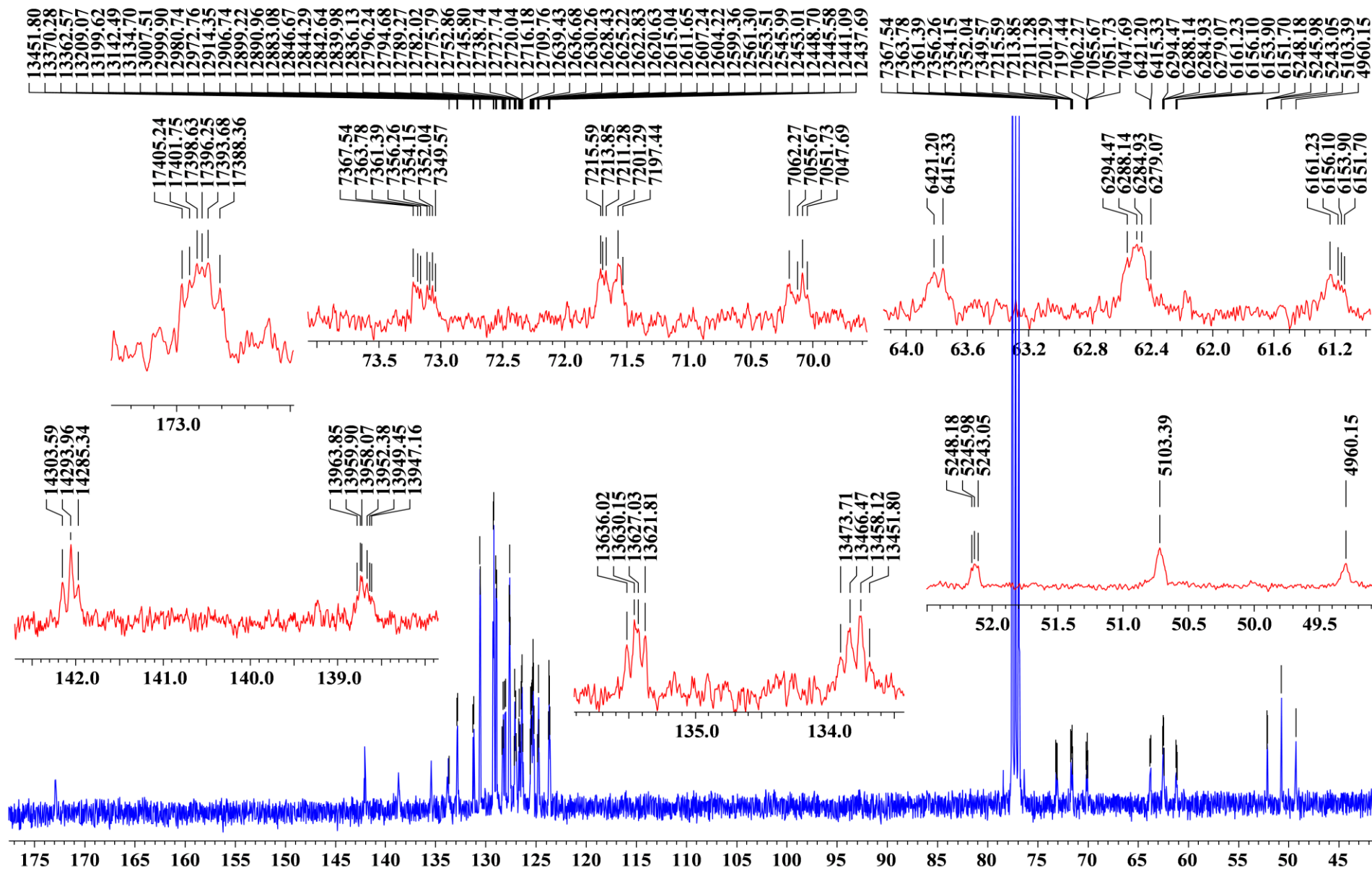


Figure S16.  $^{13}\text{C}$  NMR spectrum (100.6 MHz,  $\text{CDCl}_3$ ) of compound  $4(d_2)$ .

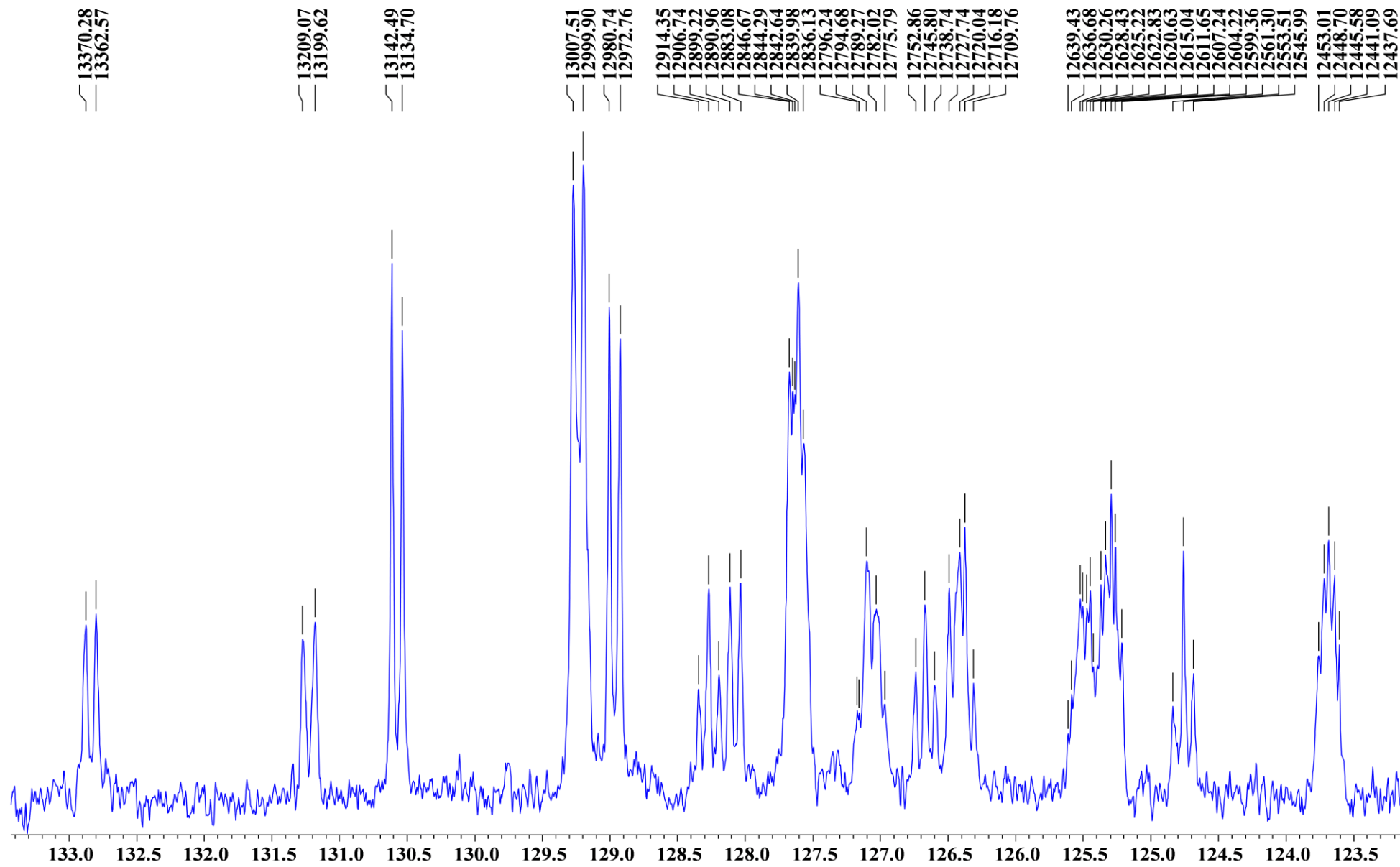


Figure S17. 123-134 ppm region of  $^{13}\text{C}$  NMR spectrum (100.6 MHz,  $\text{CDCl}_3$ ) of compound  $4(d_2)$ .

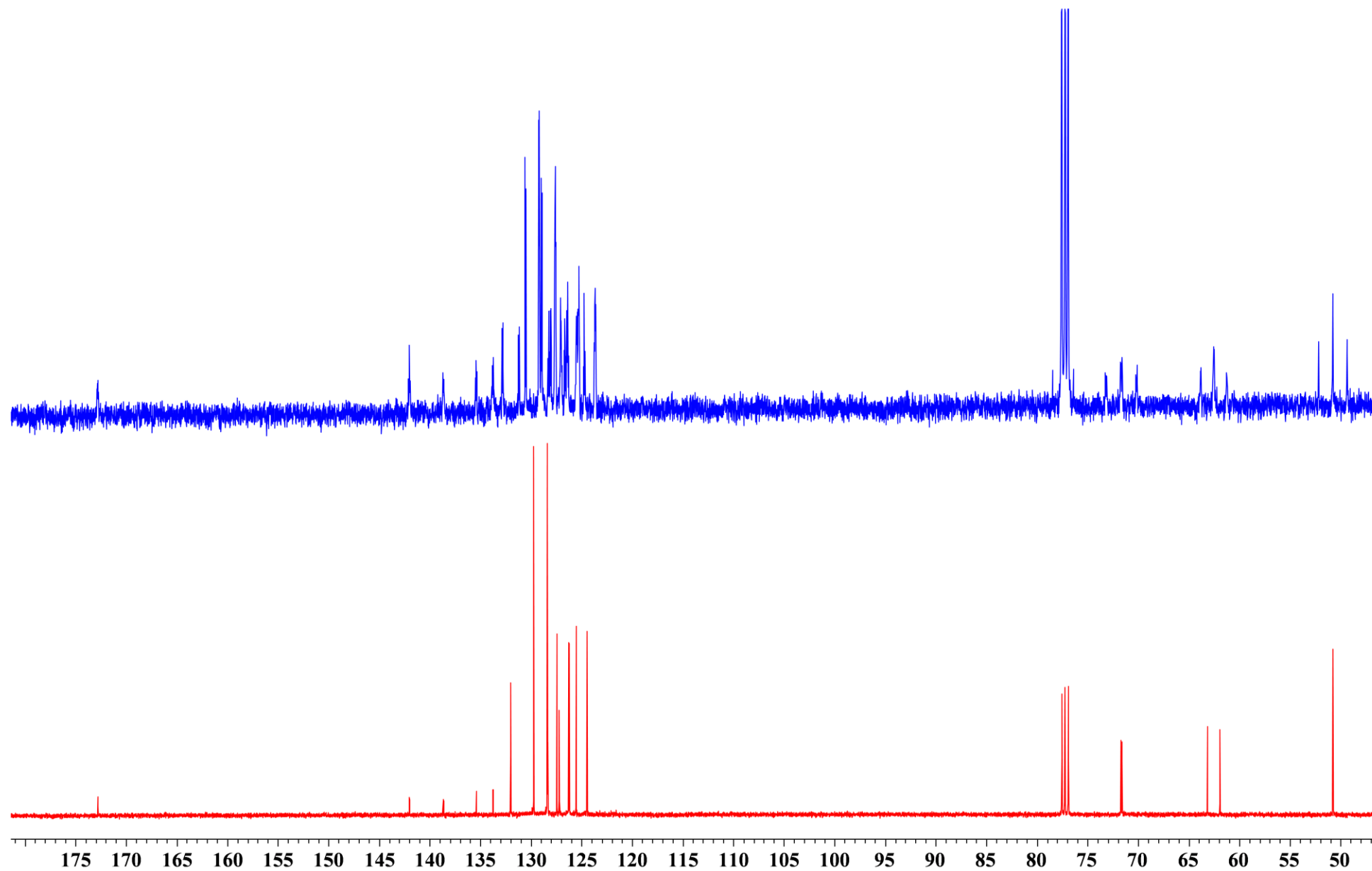


Figure S18. <sup>13</sup>C and <sup>13</sup>C-{<sup>1</sup>H} NMR spectra (100.6 MHz, CDCl<sub>3</sub>) of compound 4(d<sub>2</sub>).

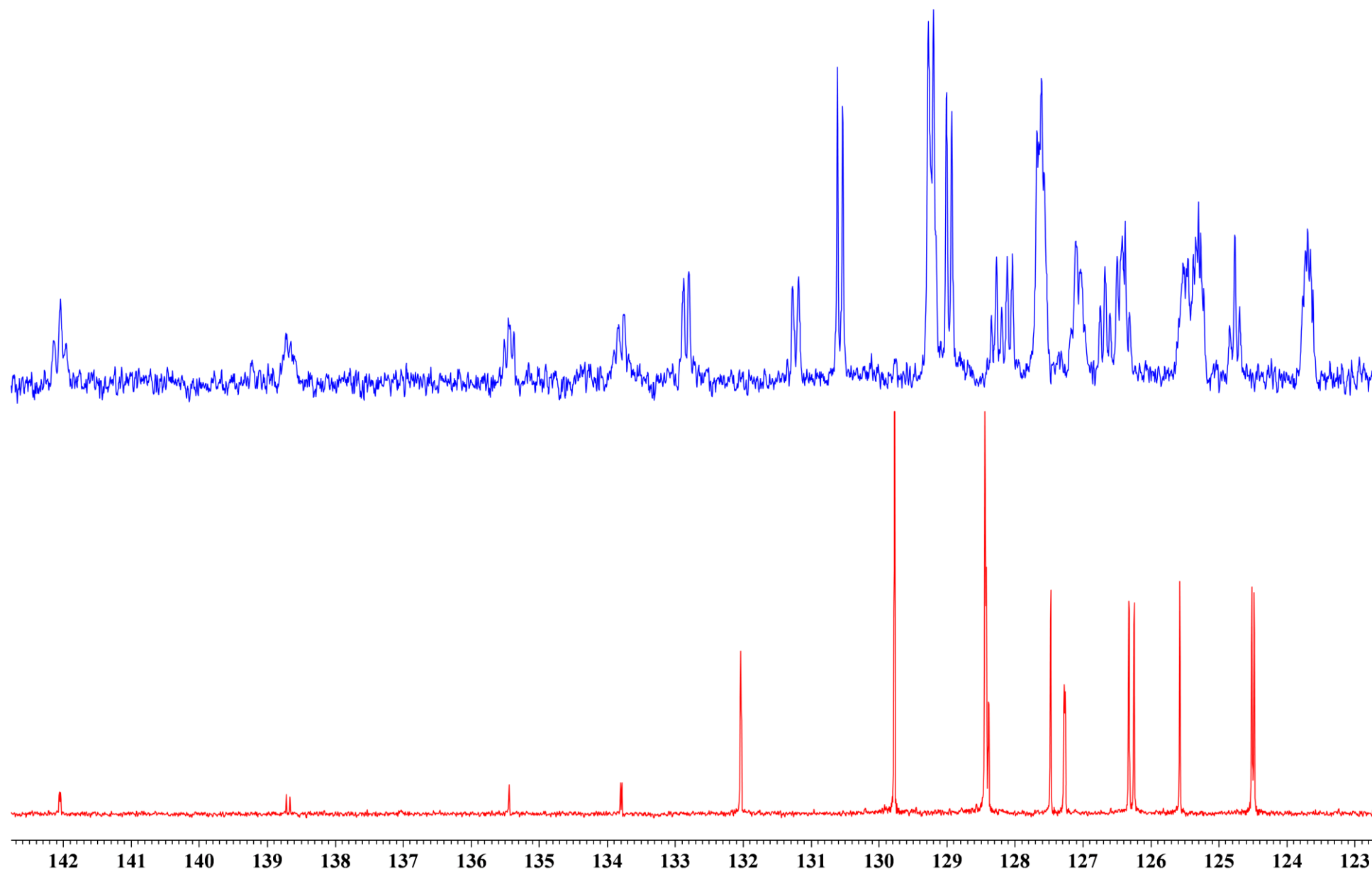


Figure S19. 123-143 ppm region of <sup>13</sup>C and <sup>13</sup>C-{<sup>1</sup>H} NMR spectra (100.6 MHz, CDCl<sub>3</sub>) of compound 4(*d*<sub>2</sub>).

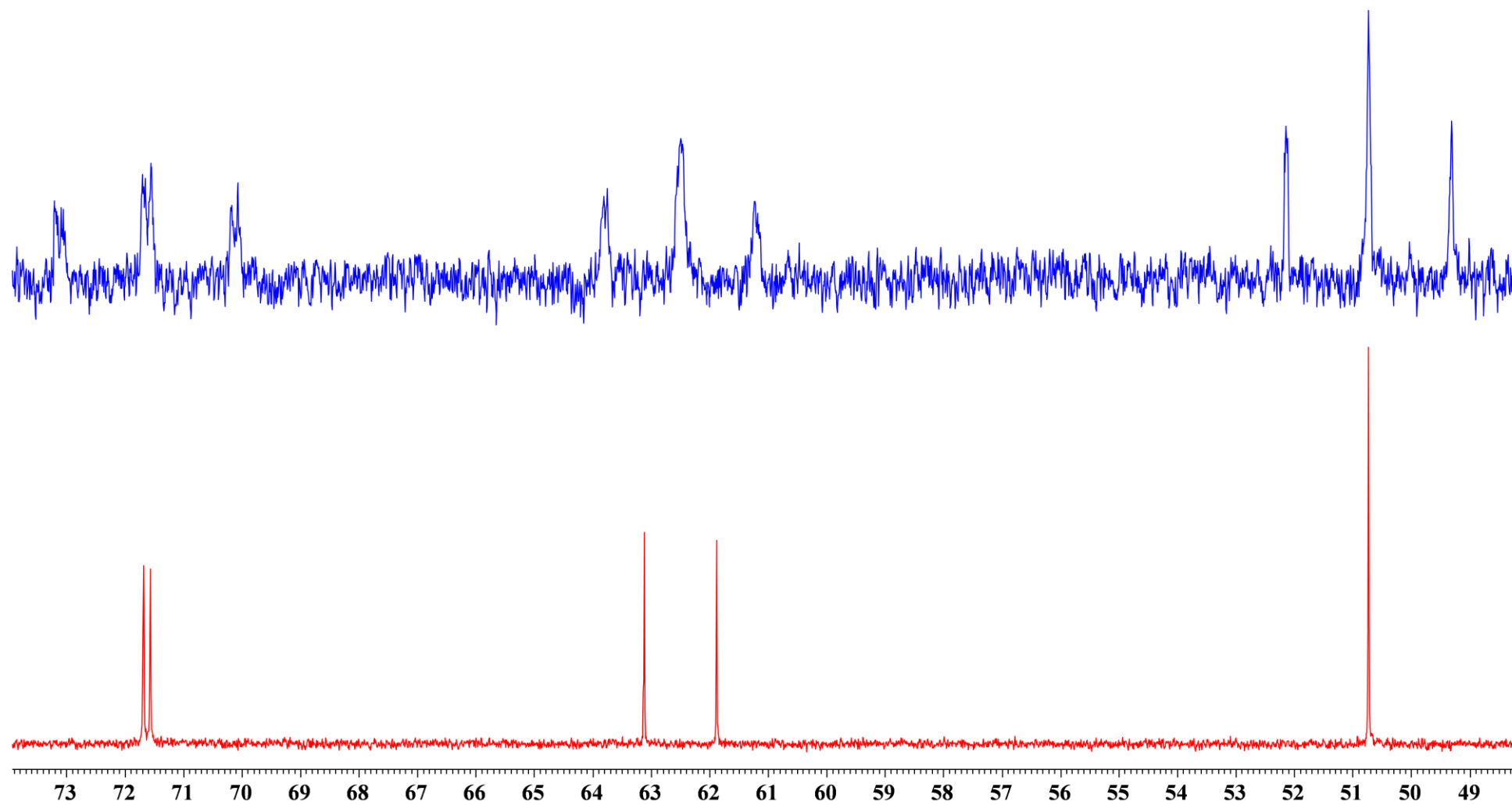


Figure S20. High-field regions of  $^{13}\text{C}$  and  $^{13}\text{C}\{-^1\text{H}\}$  NMR spectra (100.6 MHz,  $\text{CDCl}_3$ ) of compound **4**( $d_2$ ).